Ritanshu

Plag2

BTECH

Document Details

Submission ID

trn:oid:::27535:140685636

Submission Date

May 27, 2026, 10:50 PM GMT+5:30

Download Date

May 27, 2026, 10:54 PM GMT+5:30

File Name

Plag2.pdf

File Size

2.4 MB

37 Pages

9,064 Words

51,711 Characters

3% Overall Similarity

The combined total of all matches, including overlapping sources, for each database.

Filtered from the Report

- Bibliography
- Small Matches (less than 12 words)

Match Groups

11 Not Cited or Quoted 2%
Matches with neither in-text citation nor quotation marks

5 Missing Quotations 1%
Matches that are still very similar to source material

0 Missing Citation 0%
Matches that have quotation marks, but no in-text citation

0 Cited and Quoted 0%
Matches with in-text citation present, but no quotation marks

Top Sources

3% Internet sources
2% Publications
3% Submitted works (Student Papers)

Integrity Flags

0 Integrity Flags for Review

Our system's algorithms look deeply at a document for any inconsistencies that would set it apart from a normal submission. If we notice something strange, we flag it for you to review.

A Flag is not necessarily an indicator of a problem. However, we'd recommend you focus your attention there for further review.

Match Groups

11 Not Cited or Quoted 2%
Matches with neither in-text citation nor quotation marks

5 Missing Quotations 1%
Matches that are still very similar to source material

0 Missing Citation 0%
Matches that have quotation marks, but no in-text citation

0 Cited and Quoted 0%
Matches with in-text citation present, but no quotation marks

Top Sources

3% Internet sources
2% Publications
3% Submitted works (Student Papers)

Top Sources

The sources with the highest number of matches within the submission. Overlapping sources will not be displayed.

1 Student papers
University of South Africa on 2026-05-18 <1%

2 Publication
Armstrong, A.. "The Layered Intercalation Compounds Li(Mn"1"-"yCo"y)O"2: Posit... <1%

3 Internet
theses.hal.science <1%

4 Internet
www.jstage.jst.go.jp <1%

5 Student papers
Imperial College of Science, Technology and Medicine on 2025-08-21 <1%

6 Publication
Tong Dong-Ge, Lai Qiong-Yu, Wei Ni-Ni, Ji Xiao-Yang. "Synthesis of LiCo0.3Ni0.7O2... <1%

7 Internet
etheses.whiterose.ac.uk <1%

8 Student papers
Indian Institute of Technology, Kanpur on 2026-05-21 <1%

9 Publication
Sang Jun Lee, Dong Park Lee, Inkyung Kim, Junyeong Jeon, San Moon, Gyeong He... <1%

10 Publication
Xinxin Zhao, Baosheng Liu, Jiale Yang, Jiaojiao Hou, Yixin Wang, Yilong Zhu. "Synt... <1%

11 Student papers

University of the Western Cape on 2021-11-04 <1%

12 Publication

Yu Zhou, Xianhua Hou, Kaixiang Shen, Shaofeng Wang, Fuming Chen, Yajie Li, He... <1%

13 Publication

Gaole Dai, Hongjuan Du, ShanShan Wang, Jiali Cao, Min Yu, Yanbin Chen, Yuefeng... <1%

14 Internet

dr.ntu.edu.sg <1%

15 Internet

iopscience.iop.org <1%

16 Internet

www.mdpi.com <1%

CHAPTER 1

INTRODUCTION: Background and Motivation

1.1 Energy Storage Demands and the Rise of Lithium-Ion Batteries

In the recent world the increasing demand for clean and sustainable energy along with the accelerating depletion of fossil fuel reserves and the urgent need to make climate change less painful has motivated the researchers to research into advanced energy storage technologies, also the various renewable energy sources like solar and wind power produce not so continuous and unpredictable power outputs that cannot be directly matched to consumption patterns. Therefore this fundamental mismatch demands the development of efficient and cost-effective energy storage systems that are capable of varying supply-demand fluctuations and enabling grid-level energy management[1]. Also among the diverse range of electrochemical energy storage technologies currently under investigation, lithium-ion batteries have came out as the technology of choice, owing to their high operating voltage, superior gravimetric and volumetric energy densities, excellent cycle life, and low self-discharge rates compared to competing battery chemistries [2], [3], [4], [5].

1.2 The Cathode as the Performance-Limiting Electrode

Despite the remarkable commercial success of LIBs in electronics vehicles and the energy density of current state-of-the-art cell chemistries remains insufficient to meet the stringent requirements of long-range electromobility and large-scale stationary storage. The performance ceiling of a LIB is predominantly governed by the cathode material, which is the electrochemically limiting electrode in terms of both specific capacity and operating voltage[4], [5]. Over the past two decades, a broad spectrum of cathode materials has been successfully commercialized, including the layered oxide $LiCoO_2$, the spinel $LiMn_2O_4$, the olivine $LiFePO_4$, and the ternary layered compounds $LiNi_{1/3}Mn_{1/3}Co_{1/3}O_2$ (NMC111) and $LiNi_{0.8}Co_{0.15}Al_{0.05}O_2$ (NCA)[5] .

1.3 NMC622: A High-Promise Candidate in the Nickel-Rich Landscape

As the Ni content is the primary source to achieve the higher specific capacities in the NMC layered oxide family and as the cobalt is expensive and poisonous [4] and hence NMC622 offers an important way in this compositional landscape by giving a practical discharge capacity of 180-200 mAh g^{-1} and the superior thermal stability and rate capability. Also it can be seen that the structure of this cathode is (space group R-3m) where the Li^+ ions stays in the interslab space between edge-sharing MO_6 octahedral layers and thus it enable the facile two-dimensional Li^+ transport. Nevertheless, Ni-rich NMC cathodes are susceptible to a number of well-documented degradation mechanisms that limit their practical implementation. Chief among these is the Li^+/Ni^{2+} cation mixing phenomenon, whereby Ni^{2+} ions (ionic radius: 0.690 Å), owing to their close size match with Li^+ (0.760 Å), partially occupy lithium crystallographic sites and obstruct Li^+ diffusion pathways [6], [7]. Additionally, anisotropic volume changes during repeated charge-discharge cycling induce microcracks within secondary particles, exposing fresh surfaces to electrolyte attack, accelerating impedance growth, and precipitating capacity fade [7].

1.4 Degradation Mechanisms in Ni-Rich NMC Cathodes

Cationic substitution at the transition metal sites has been established as one of the most effective and practically viable strategies to overcome these limitations. Judicious selection of a dopant ion with appropriate ionic radius, oxidation state, and metal-oxygen bond strength can simultaneously suppress cation disorder, expand the Li^+ diffusion slab spacing, reinforce the structural framework against volume change, and improve electronic conductivity.

1.5 Why Chromium? Rationale for Cr^{3+} Substitution in NMC622

Among the candidate dopants explored in the literature - including Ti^{4+}, Mg^{2+}, Zr^{4+}, Mo^{6+}, Fe^{3+}, and Al^{3+} , chromium (Cr^{3+}) presents a particularly compelling combination of properties[6] as it has an ionic radius of 0.615 Å and also it is closely equal with the ionic radius of Ni^{3+}(0.561 Å) and Co^{3+} (0.611 Å) and hence the substitution of these two or any one gives minimal structural degradation[8]. Also it can be seen that the Cr-O bond dissociation energy is significantly higher than that of Ni-O and Co-O so

the substitution by Cr^{3+} reduce the oxygen release at elevated potentials, and enhance the thermodynamic stability of the host lattice[8], also the d^3 electronic configuration of Cr^{3+} where it has three unpaired electrons occupy the t_{2g} orbitals of the octahedral crystal field and hence therefore it is minimally disruptive to the electronic structure of the NMC host and do potentially gives a improved charge delocalization[8], [9].

1.6 Scope and Objectives of the Present Work

As seen in the various literature the Cr doping has an positive impact in NMC cathode systems as it provide better structural evolution, morphological uniformity and bonding characteristics also multi-technique electrochemical performance across a controlled doping range[8], so in this work, Cr-doped NMC622 cathode materials with nominal compositions $LiNi_{0.59}Cr_{0.01}Mn_{0.2}Co_{0.2}O_2$ (1% Cr), $LiNi_{0.57}Cr_{0.03}Mn_{0.2}Co_{0.2}O_2$ (3% Cr), and $LiNi_{0.55}Cr_{0.05}Mn_{0.2}Co_{0.2}O_2$ (5% Cr) were synthesized via a citrate-assisted sol-gel method because of its ability to achieve molecular-level homogeneity of the precursor mixture and precise control over particle nucleation and growth[10], [11]. And after that he synthesized materials were used for the structural and morphological characterization using XRD and SEM to evaluate phase purity, lattice parameter evolution and particle morphology and along with that electrochemical performance was systematically assessed through GCD to study the long-term capacity retention and specific capacity. After that the results reveal that doped cathode material shows better structural order and better cycling stability relative to the undoped NMC622.

The findings of this study are looking to provide meaningful design principles for the development of structurally stable, high-performance Ni-rich cathode materials for upcoming LIBs.

CHAPTER 2

LITERATURE REVIEW

2.1 Development of Intercalation type cathode materials

Lithium-ion batteries are largely recognised as the leading technology for energy storage devices. Research interest has widely grown in recent years in this field due to its good cycling performance and low irreversible capacity. It still leaves a gap for further research due to the key challenges like high cost, safety performance, stability, cycle life and effective recycling strategies[12]. Professor John B. Goodenough played a significant role in the field of rechargeable batteries. He discovered 1st generation layered-type(2-D) lithium cobalt oxide ($LiCoO_2$) in 1980. Further he also discovered the second generation spinel-type(3-D) lithium manganese oxide (LiMn2O4) in 1981 and 3rd generation olivine-type(1-D) lithium iron phosphate (LiFePO4) in 1997. Each of these cathodes have their pros and cons.1st gen layered-type $LiCoO_2$ has the highest capacity of 274 mAh/g enabling fast Li^+ diffusion and excellent cycling stability but it suffers from structural instability, low irreversible capacity and toxicity concerns.[13] Also the high cost of Co and it's toxicity lead Goodenough to find some other alternative for cathode material In 1981 he along with M. Thackeray et al discovered the manganese spinel $LiMn_2O_4$ as a cathode for lithium insertion. Although spinel-type cathode with three dimensional structure offers high rate capability, enhanced safety, good structural stability, thermal stability, and low cost, it however has certain drawbacks like limited practical capacity, high voltage instability and most important the phase transformation from cubic to tetragonal due to the Jahn-Teller effect that occur during charging and discharging and it leads to the capacity fade after approx. 300 cycles[14].

Then comes the olivine-type cathode material inspired by polyanion oxide "inductive effects" that contain XO_4 tetrahedral anion structural units. It offers good thermal stability and safety without oxygen release due to a strong covalent bond that exists between all oxygen and P^{5+} to form tetrahedral $PO4^{3-}$ structural unit.

The structure of these three cathode material is given below in the figure for comparison.

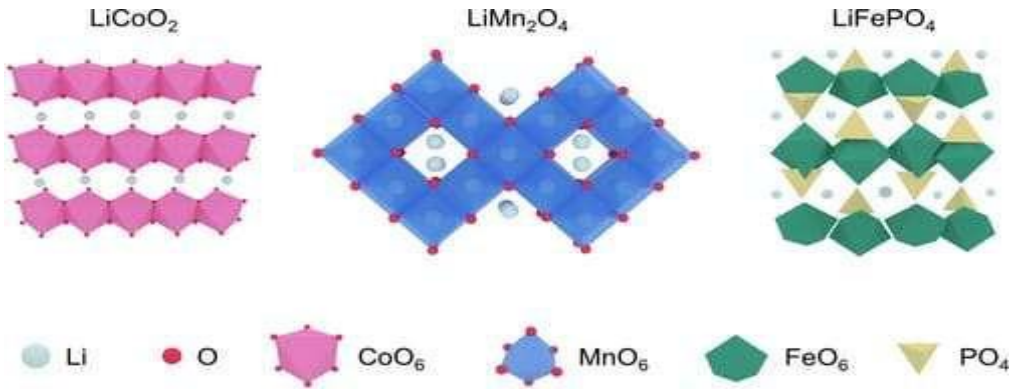

Fig:1 Different type of cathode material

2.2 Review of NMC cathode material

Recently NMC cathode materials have been a topic of wide interest in the field of lithium ion batteries owning to their greater specific capacity. Early stage NMC typically included approximately 33% Nickel and then the content of Nickel is increased in subsequent generations having 80% Nickel content in case of NMC811.However higher Nickel content in NMC811 requires specialized oxidation processes. NMC cathodes evolved to maximize Ni for capacity, Mn for lowering internal resistance by stabilizing the lithium-ion diffusion pathways and Co for improving cycling stability.[12] NMC622 cathode is widely used for lithium-ion battery due to its optimal balance of high energy density, cost-effectiveness and thermal stability, and compared to alternatives like NMC111 or NMC811. However, NMC622 have some well know limitations like cation mixing between Li^+ and Ni^+ ions, interfacial instability at high operating voltage and structural degradation during long-term cycling, thereby restricting the material's practical rate performance and

cycle life[15]. To overcome these issues various doping and ion substitution techniques are actively explored by various researchers and various modifications strategies have also been reported in the literature. These strategies involve bulk doping by various metal ions, surface coating by various metal oxides and structural techniques through composition control[16]. Although these strategies have showing some positive results it still leaves the room for more effective and scalable solutions.

Several dopant elements have been investigated for layered oxide like Al, Ti, Mg, Zr, Nd, Na, Cr, and Fe and their effect have been studied and they have shown promising result comparatively with pristine[17]. For example, Magnesium doping has show the improvement in the structural stability of the cathode material by suppressing the oxygen loss and also by reducing the lattice distortion during cycling [18] and in the same manner aluminum doping also have shown to enhance the thermal stability because of the strong Al-O bonds that it make with the oxygen and hence help to stabilize the oxygen framework within the layered lattice [19]. Also many Rare-earth dopants such as neodymium have also shown the ability to improve cycling retention through stabilization of grain boundaries and suppression of microcrack formation [20].

Taking in consideration the different dopants investigated and studied so far in NMC, chromium has maintain to attract the significant interest because of it has strong bonding interaction with oxygen and it has the ability to stabilize the layered oxide structures during electrochemical cycling [21]. Apart from that Chromium doping also has been reported to reduce the transition metal migration, suppress structural distortion, and to improve cycling stability in several layered cathode systems [22] and unlike the other elements like nickel, chromium also does not contribute substantially

towards the electrochemical capacity directly, also its tendency to stabilize the structure can significantly improve long-term electrochemical performance and because of this stabilization effect of chromium which is mainly associated with the strong Cr-O covalent interaction within the transition metal layer it suppresses oxygen release during high-voltage charging and hence reduces the structural collapse of the layered framework [23]. Apart from that the chromium substitution can also reduce the concentration of unstable Ni^{2+} ions within the lattice and hence it can decrease the probability of cation mixing during repeated cycling of the cathode material[23].

Despite all the considerable progress in the cathode materials there are still several key challenges for example balancing the high energy density along with the structural stability is still very difficult and that too especially in Ni-rich cathodes or system where if we try to increase the concentration of the nickel it accelerates the degradation even though it improves the capacity. And that's why improving the thermal safety of the cell without sacrificing the electrochemical performance of the material is still a major research objective.

So because of these challenges in our current research we are focusing on the various modification strategies like the Cr doping in NMC622 cathode, synthesis route and microstructural control and hence our aim is to supress the degradation mechanism while maintain the high reversible capacity and long term cycling stability unlike the pristine NMC622 cathode material.

CHAPTER 3

EXPERIMENTAL

3.1 Material and Reagents

Lithium acetate dihydrate ($LiCH_3COO \cdot 2H_2O$) with purity 99.9%, Chromium acetate(II) hydrate $Cr_2(CH_3CO_2)_4(H_2O)_2$ with purity 99.0%, nickel(II) acetate tetrahydrate $(Ni(CH_3COO)_2 \cdot 4H_2O$ with purity 98.0%, Manganese(II) acetate tetrahydrate ($Mn(CH_3COO)_2 \cdot 4H_2O$) with purity 990% and Cobalt(II) acetate ($Co(CH_3COO)_2 \cdot 4H_2O$) with purity 98.0% were purchased from Sigma-Aldrich. Citric acid ($C_6H_8O_7 \cdot H_2O$, 99.9%) served as the chelating agent, also obtained from Sigma-Aldrich. Deionized water (DI) were employed as solvent.

3.2 SYNTHESIS METHODS

3.2.1 Synthesis of Pristine and Cr-Doped NMC622 Cathode Materials

Pristine NMC622 and chromium-doped NMC622 cathode materials with nominal compositions $LiNi_{0.6}Mn_{0.2}Co_{0.2}O_2$, $LiNi_{0.59}Cr_{0.01}Mn_{0.2}Co_{0.2}O_2$ (1% Cr), $LiNi_{0.57}Cr_{0.03}Mn_{0.2}Co_{0.2}O_2$ (3% Cr), and $LiNi_{0.55}Cr_{0.05}Mn_{0.2}Co_{0.2}O_2$ (5% Cr) were synthesized via a citrate-assisted sol-gel method. Stoichiometric quantities of nickel, manganese and cobalt acetate tetrahydrate, and chromium precursor were dissolved separately in deionized water according to the desired stoichiometric ratios. The nickel precursor solution was prepared in a 100 mL beaker, while manganese and cobalt precursor solutions were prepared separately and stirred at 350 rpm and 80°C for 1 h to achieve homogeneous dissolution. Lithium acetate dihydrate was dissolved separately in DI water and thoroughly mixed. Subsequently, all precursor solutions were combined and continuously stirred at 300-350 rpm within the temperature range of 60-80°C. Citric acid monohydrate was dissolved separately and added to the mixed precursor solution as a chelating agent to facilitate homogeneous cation distribution and stable complex formation. The resulting solution was heated and stirred continuously at 90-100°C for several hours until a transparent viscous gel was obtained. The formed gel was vacuum dried at 130° C for 12-15 h. The dried precursor

material was then pre-calcined at 500° C for 5 h in air atmosphere to remove residual organics and promote precursor decomposition and then finely ground using an agate mortar and pestle to ensure compositional homogeneity and calcined at 900°C for 12 h in air atmosphere to obtain the final layered Cr-doped NMC622 cathode materials. After completion of calcination, the furnace was allowed to cool naturally to below 50°C before collecting the synthesized powders for structural, morphological, and electrochemical characterization.

3.3 Physical characterization

3.3.1 Structural and Morphological Characterization

The phase purity and crystal structure of the synthesized pristine and Cr-doped NMC622 cathode materials were investigated using XRD analysis with Cu-Kα radiation (λ = 1.5406, Å) [6]. The diffraction measurements were carried out over the 2θ range of 10°-90° in Bragg-Brentano reflection geometry[5]. The obtained diffraction patterns were indexed according to the layered α-$NaFeO_2$-type structure with rhombohedral $R\bar{3}m$ symmetry[7]. The structural evolution upon chromium incorporation, phase purity, peak splitting behavior, crystallinity, and cation mixing characteristics were analyzed from the XRD data.

The surface morphology, particle distribution, and microstructural characteristics of the synthesized materials were examined using FESEM. The particle size distribution and agglomeration behavior were analyzed to understand the effect of Cr substitution on particle growth and morphological uniformity[7], [14].

Elemental composition and transition-metal distribution within the synthesized cathode materials were investigated using EDX attached to the FESEM instrument. The EDX analysis was performed to confirm the presence and relative distribution of Ni, Mn, Co, Cr, and O elements in the synthesized samples[8].

3.4 Electrochemical Measurement

3.4.1 Electrode preparation

The electrochemical electrodes were prepared using pristine and Cr-doped NMC622 cathode materials as the active material. The active cathode material, carbon black and PVDF as were mixed in a weight ratio of 8:1:1 and dispersed in NMP to form a homogeneous slurry. Specific volume of NMP was added to dissolve the binder. After that the slurry was placed on a magnetic stirrer for few hours to get a well-mixed slurry and casted on an aluminium foil using a doctor-blade to spread with thickness of 10mm and the resulting mixture was uniformly coated onto aluminum foil, serving as the current collector, and subsequently dried at 90 °C for 11-12 h. After drying, circular electrode discs with appropriate diameter were punched from the coated aluminium foil and then the electrode was vacuum dried in a oven at 120 °C to remove residual solvent. After that the electrode were used directly for electrochemical cell assembly.

Table 1: Electrode slurry composition

Component	Weight Percentage	Mass (g)
Active Material (A.M)	80%	0.24 g
Activated Carbon (A.C)	10%	0.03 g
Polyvinylidene Fluoride (PVDF)	10%	0.03 g
Solvent	—	NMP (N-Methyl-2-pyrrolidone)

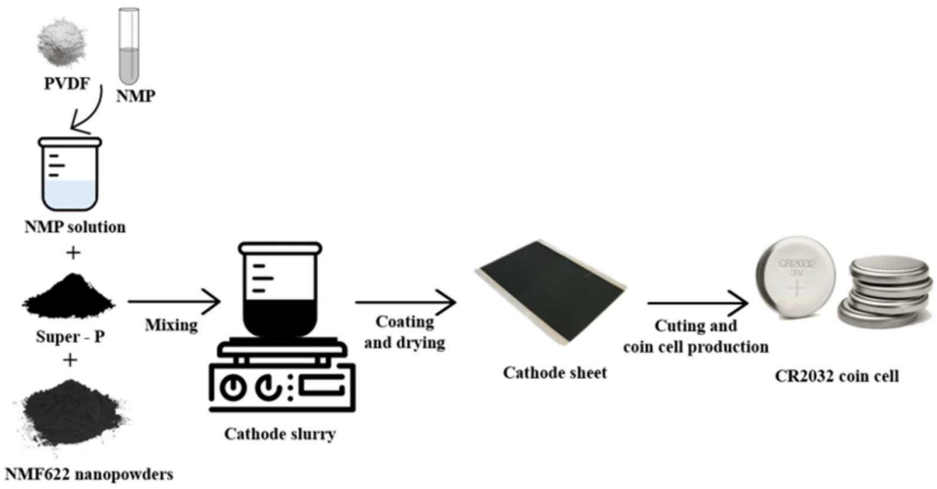

Figure 2: Schematic representation of stepwise synthesis of slurry

3.4.2 Coin Cell Assembly

The CR2032-type coin cell was assembled inside an argon-filled glovebox. The prepared NMC622 and Cr-doped NMC622 electrode (diameter: 9 mm; active area: 0.64 cm^2; mass loading ≈ 2.5 mg cm^{-2}) served as the working electrode, while two lithium metal electrodes (diameter: 10 mm) functioned as counter and reference electrodes. A 1 M $LiPF_6$ solution in a EC:DMC(1:1) wt./wt was used as the electrolyte and a polypropylene separator was placed between the electrodes.

3.4.3 Galvanostatic Charge-Discharge Measurements

9

GCD measurements were carried out at room temperature within the voltage range of 2.5-4.5 V (vs. Li/Li^+). The rate performance measurements were conducted sequentially with 5 cycles at 0.1C to evaluate capacity retention and structural stability during repeated lithiation/delithiation processes.

15

CHAPTER 4

RESULTS AND DISCUSSION

4.1. XRD Analysis

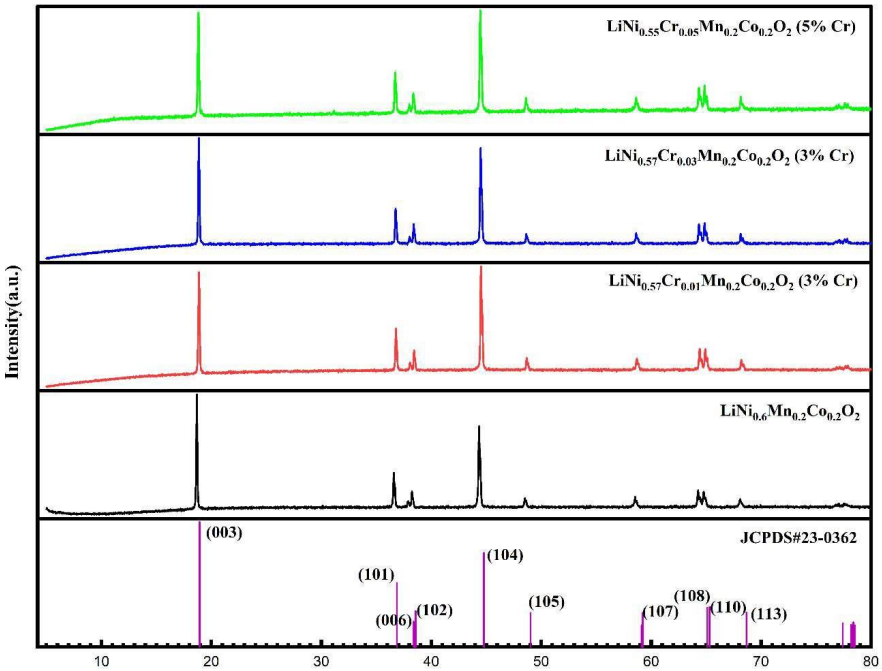

Figure 3: XRD pattern of $LiNi_{0.6}Mn_{0.2}Co_{0.2}O_2$ and $LiNi_{0.6-x}Cr_xMn_{0.2}Co_{0.2}O_2$ along with JCPDS

The XRD patterns of pristine and Cr-doped NMC622 cathode materials shows the successful formation of a layered α-$NaFeO_2$-type hexagonal structure with rhombohedral $R\bar{3}m$ symmetry, in agreement with the standard JCPDS No. 23-0362 reference [8]. All principal reflections can be indexed to the layered NMC phase, including the (003), (101), (006), (102), (104), (105), (107), (108), (110), and (113) planes, which is the typical fingerprint of well-crystallized layered lithium transition-metal oxides [6]. The absence of extra reflections suggests that no detectable impurity

phases were formed during synthesis, indicating that chromium incorporation did not disrupt the parent lattice in a way that produced separate crystalline by-products[24].

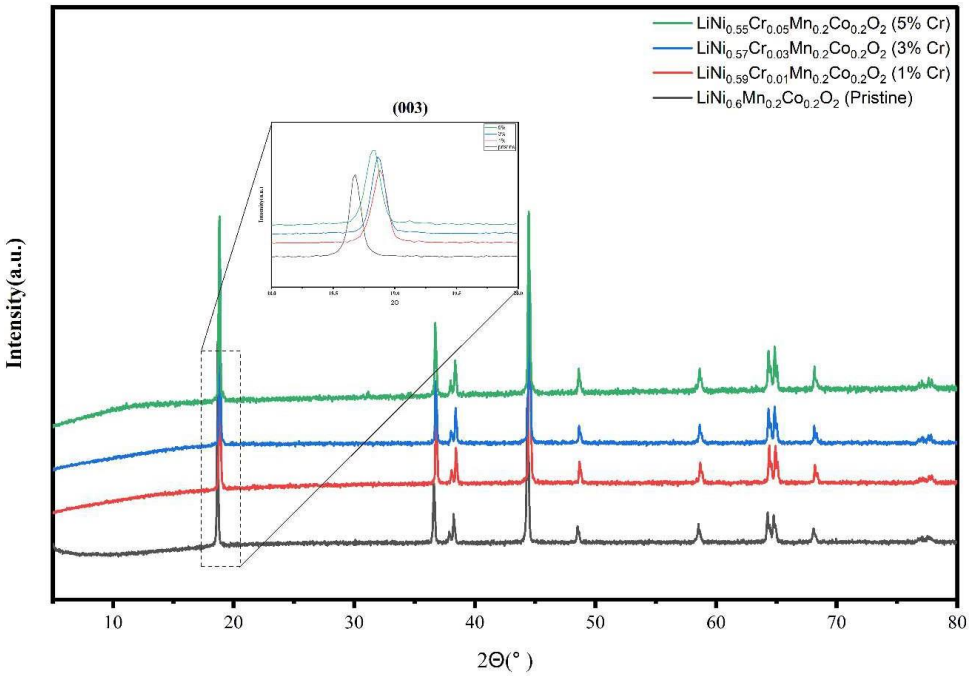

Figure 4: XRD pattern of $LiNi_{0.6}Mn_{0.2}Co_{0.2}O_2$ and $LiNi_{0.6-x}Cr_xMn_{0.2}Co_{0.2}O_2$

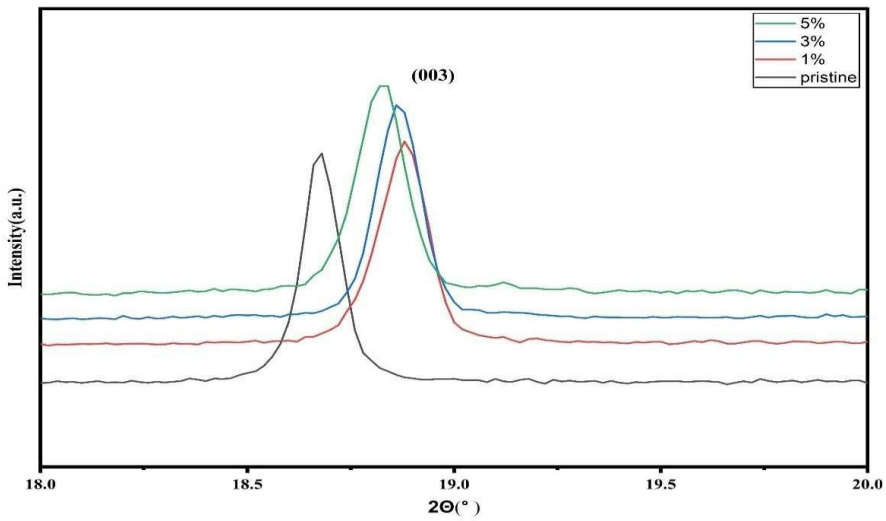

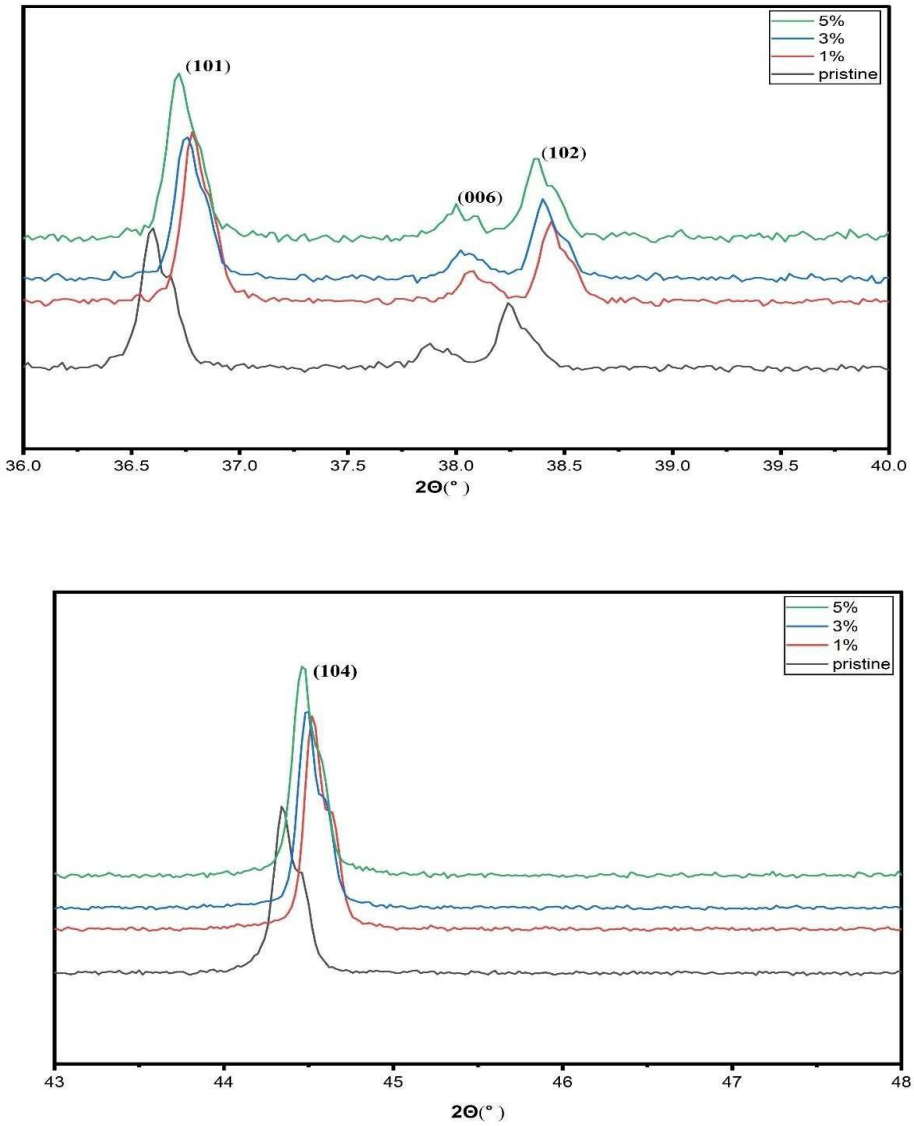

Figure 5: Shifting in peaks (a) (003), (b) (101) and (c) (104)

13

As seen in the above enlarged graphs the splitting of the (006)/(102) and (108)/(110) peaks shows a good layered structure along with the good hexagonal ordering and relatively low structural disorder [25], also it can be seen that in layered $R\bar{3}m$ materials we use these pairs of peak as a structural check as their resolution usually depends on the effect of the long-range ordering within the layered lattice [24]. Also it can be seen

that as the structure is more ordered then the reflections are better separated and when there is any kind of disorder like increase in phase degradation then the peaks tend to merge or broaden indicating worse layered structure [26], so it can be interpret that the observed splitting show that the synthesized powders have the characteristic layered framework that is expected in the high-quality NMC cathodes.

Table 2: 2 Theta shift in each peak

	(003)	(101)	(006)	(102)	(104)	(105)	(107)	(108)	(110)	(113)
Pristine	18.68	36.60	37.88	38.24	44.34	48.62	58.54	64.26	64.78	68.08
1%	18.88	36.78	38.08	38.44	44.52	48.64	58.70	64.42	64.92	68.20
3%	18.86	36.76	38.02	38.40	44.50	48.68	58.64	64.34	64.86	68.14
5%	18.84	36.72	38.00	38.38	44.46	48.52	58.64	64.34	64.86	68.16

Also as it can be seen that there is a systematic shift of the diffraction peaks towards the higher 2θ values for the Cr-doped samples relative to pristine NMC622 [8], for example, the (003) reflection shifts from 18.68° in the pristine material to 18.88°, 18.86°, and 18.84° for 1%, 3% and 5% Cr, respectively, while the (104) reflection shifts from 44.34° to 44.52°, 44.50° and 44.46°. Such type of shifting in the right direction is also observed for the remaining indexed peaks which can be related to the effect of Cr doping and it is also systematic rather than accidental shifting of the peaks [7]. As we know that according to Bragg's law the higher the diffraction angle the smaller will be the interplanar spacing and that's why this trend shows a medium lattice contraction after chromium incorporation, also in practical terms we can also say that Cr is kind of modifying the average crystal spacing of the layered framework which is also a good indicator of structural modification of the undoped cathode material instead of an unchanged pristine lattice [1], [8]. Also the reason of the peaks shift is due to the fact that doping do changes the local crystal chemistry of the TM layer[27] and in our case the chromium substitution changes the average bond lengths, and the local bonding environment and these changes can be seen in the peak positions in the XRD. As we know that in the layered NMC cathodes due to the cation distribution even a small change can be seen in the transition-metal sublattice and it

can influence the lattice parameter and the oxygen framework because the structure is relatively sensitive [6] so the observed shifts in the peak in our case shows that chromium is not simply physically mixed with the powder but it is also affecting the host lattice itself and that is why even a slight shift in the peak are structurally meaningful for the study of material. As it can be seen that the peak shifting can be smaller again at higher Cr concentration and it is therefore physically reasonable [6], also as several competing processes happen at the same time the doping effects are not always linear and hence the lattice contraction from substitution can be seen along with the cation redistribution, and possible microstructural inhomogeneity and that's why at low to moderate doping, the lattice may respond mainly through contraction and stabilization but at higher doping level the local distortion can be relax a lil bit or it can be said that it will be compensated by defects which reduces the net shift observed in the diffraction pattern [7], so the less shift at higher Cr concentration does not mean that the dopant is ineffective but it can be said that the structural response is reaching a balance point.

The intensity ratio $I_{(003)}/I_{(104)}$ provides another important structural clue. This ratio is commonly used to assess cation mixing in layered NMC cathodes, since the (003) reflection is sensitive to ordering between lithium and transition-metal layers, while the (104) reflection is less sensitive to that mixing. Our values change from 1.184 for pristine to 0.972 for 1% Cr, 1.047 for 3% Cr, and 0.989 for 5% Cr . The trend suggests that chromium modifies the cation distribution and layered ordering, with 3% Cr showing the most balanced response among the doped compositions . Here while discussing, notice that this ratio is a qualitative indicator rather than an absolute measure of performance, but it still strongly supports the conclusion that Cr changes the crystal chemistry of the cathode [29].

This also addresses the question of whether a larger d-spacing in the pristine sample automatically means better lithium transport[2], [3]. The answer is no, because lithium-ion transport in layered cathodes depends on more than just interlayer distance and the cation mixing, defect chemistry and structural stability along with other effects can all show a small difference in geometric spacing during the cycling process, so it can be said that even tho the pristine sample can have a little bit of larger interplanar

spacing still the Cr-doped samples can somehow still show better electrochemical behavior if somehow the doping reduces the effect of cation disorder and stabilizes the lattice[2] and also if the d-spacing is smaller then it does not mean that the Li^+ exchange in the material is poor but the overall diffusion environment can still somehow actually improve if the structure becomes more ordered and more stable in the cathode material[30]. Also the XRD results show that chromium doping modifies the NMC622 lattice without destroying the layered phase and the pattern remains with phase purity and the layered doublets can be seen and also the peak positions shift systematically, and the intensity ratio changes with composition [25] so if all these are taken together then these features do show the successful structural incorporation of Cr and confirm that the dopant is influencing the host lattice in a controlled manner[25] and so the data is supporting the idea that moderate Cr doping is beneficial for electrochemical cycling, rate capability, and impedance behavior, which should be discussed together with the GCD results in the upcoming chapters[26].

14

Table 3: Intensity ratio of (003) and (104) peak

	I (003)	I (104)	I (003)/I (104)
Pristine	**170**	**143.574**	**1.18406023**
1%	**174.966**	**180**	**0.9720314**
3%	**190**	**181.4**	**1.04740904**
5%	**197.852**	**200**	**0.98926149**

4.2 SEM

FE-SEM graphs of the pristine NMC622 are dense agglomerates of faceted primary crystallites with near-octahedral to polyhedral morphology and is common for layered Ni-rich NMC cathodes [31], [32]. The particles seem to be strongly fused into secondary aggregates with relatively smooth facets and only limited intergranular voids, indicating a compact microstructure rather than a highly porous one. The

individual primary particles are more obvious in the image at higher magnification, and the sharp edges and well-developed faces are indicative of good crystallization during the high temperature lithiation step [32].

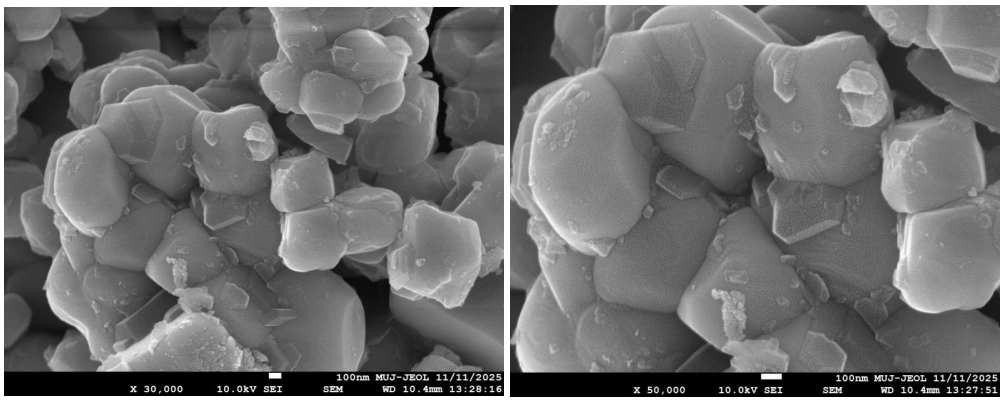

Figure 6: SEM images of (a) and (b) $LiNi_{0.6}Mn_{0.2}Co_{0.2}O_2$

Figure 6(a) and (b) displays the FE-SEM images of the pristine NMC622 displaying compact morphology[32], characteristic of layered Ni-rich cathode materials. The sample consists of agglomerated faceted primary crystallites with near-octahedral/polyhedral shapes, which are assembled into larger dense secondary particles[31]. The relatively smooth particle faces and well-defined edges suggest effective crystal growth during synthesis, while the limited interparticle porosity suggests a tightly packed microstructure [33]. Some particles show small surface fragments and irregular deposits, presumably due to particle fracture or handling during sample preparation[33]. The observed morphology is overall consistent with previously reported pristine NMC622 materials synthesized by solid-state or other synthesis routes[34].

4.3 EDX

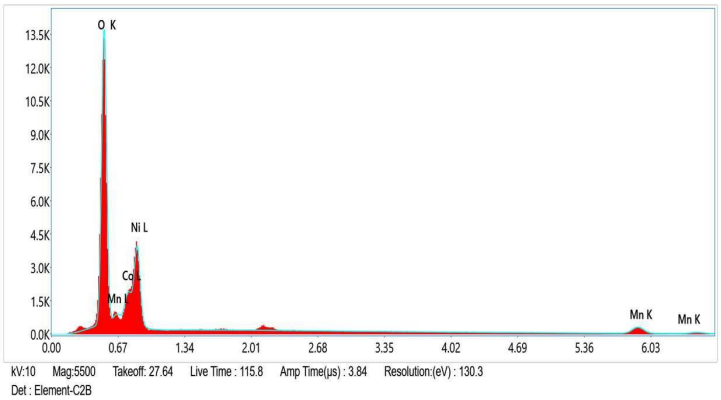

Figure 7: EDX spectrum of (a) $LiNi_{0.6}Mn_{0.2}Co_{0.2}O_2$

Table 4: Elemental composition of (a) $LiNi_{0.6}Mn_{0.2}Co_{0.2}O_2$

Element	Weight %	Atomic %	Error %
O K	37.4	68.3	6.8
Mn K	16.4	8.7	9.5
Co K	20.4	10.1	17.4
Ni K	25.8	12.9	9.9

The EDX spectrum and quantification (Figure 7, Table 4) show that the as-synthesized sample is oxygen-rich and is mainly composed of Ni, Co and Mn in proportions consistent with NMC622, oxygen dominates the signal (O K: 37.4 wt%, 68.3 at.%) and Ni, Co and Mn are detected at 25.8 wt% (12.9 at.%), 20.4 wt% (10.1 at.%) and 16.4 wt% (8.7 at.%) respectively within the instrument error reported in Table 4. The strong O K peak in the spectrum indicates the expected oxide matrix and the relative intensities of the transition-metal peaks support a Ni-rich layered oxide phase rather than a separate metal/oxide impurity phase [35]. The observed deviations from ideal stoichiometry in atomic % are within the usual uncertainty of EDX surface analysis and may reflect surface oxygen enrichment and the sampling of secondary particle facets, rather than differences in bulk composition as reported by bulk techniques like ICP-OES or XRF [33], [35]. The small high-energy background and small spectral

features are most likely due to the detector geometry and accelerating voltage conditions used for the FE-SEM/EDX mapping and do not represent additional elements beyond the NMC system[33], [34].

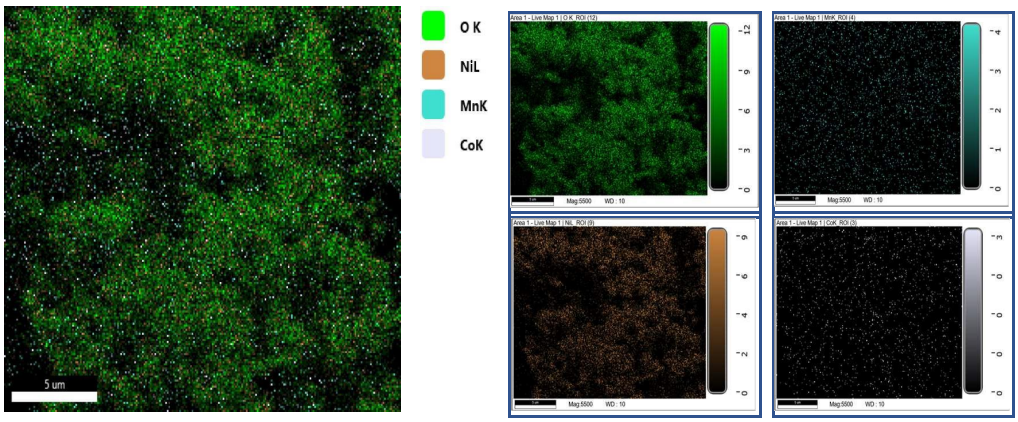

Figure 8: Elemental mapping of (a) O (b) Ni (c) Co (d) Mn

Elemental mapping of pristine LiNi0.6Co0.2Mn0.2O2 is shown in Figure 8. ,the spatial distribution of respective elements over the examined area. The maps show that all four elements are homogeneously distributed over the secondary particles, indicating a good compositional homogeneity and an efficient mixing of the transition-metal species during the synthesis. No strong elemental segregation, surface enrichment or compositionally distinct areas are observed in the mapped region, which is usually typical for well-formed NMC622 cathode powders[35]. The homogeneous elemental dispersion further supports the formation of a stable layered oxide microstructure and is in accordance with previously reported mapping results of NMC622[31]

4.3 Electrochemical Analysis

4.3.1 GCD

GCD analysis is an electrochemical characterization techniques used for evaluating lithium-ion battery materials like specific capacity and capacity retention, in this technique, the battery cell is charged and discharged at a fixed current within a selected voltage range where the variation in voltage is recorded with respect to time or specific capacity. The obtained charge–discharge curves that we get from this technique provide direct information about the lithium intercalation and deintercalation mechanism of the cell, structural stability, electrochemical reversibility, polarization behaviour and cycling performance of the electrode material [36]. Coming to layered oxide cathodes such as $LiNi_{0.6}Mn_{0.2}Co_{0.2}O_2$ (NMC622), the galvanostatic profiles generally show smooth sloping charge-discharge curves because lithium extraction and insertion occur through continuous solid-solution reactions rather than abrupt two-phase transformations [37].

In our present work, galvanostatic charge-discharge measurements were carried out for pristine and Cr-doped NMC622 cathode materials in the voltage window of 2.5-4.5 V at a C-rate of 0.1 C and the electrochemical performance of the synthesized cathodes was evaluated during the initial five cycles in order to study the influence of chromium substitution on discharge capacity, cycling stability, and reversibility of lithium-ion transport. Also it is noticed that the charge-discharge profiles of all synthesized samples displayed the characteristic electrochemical behaviour associated with layered α-$NaFeO_2$-type cathodes, indicating that the layered crystal structure remained preserved even after chromium incorporation into the transition metal layer [38].

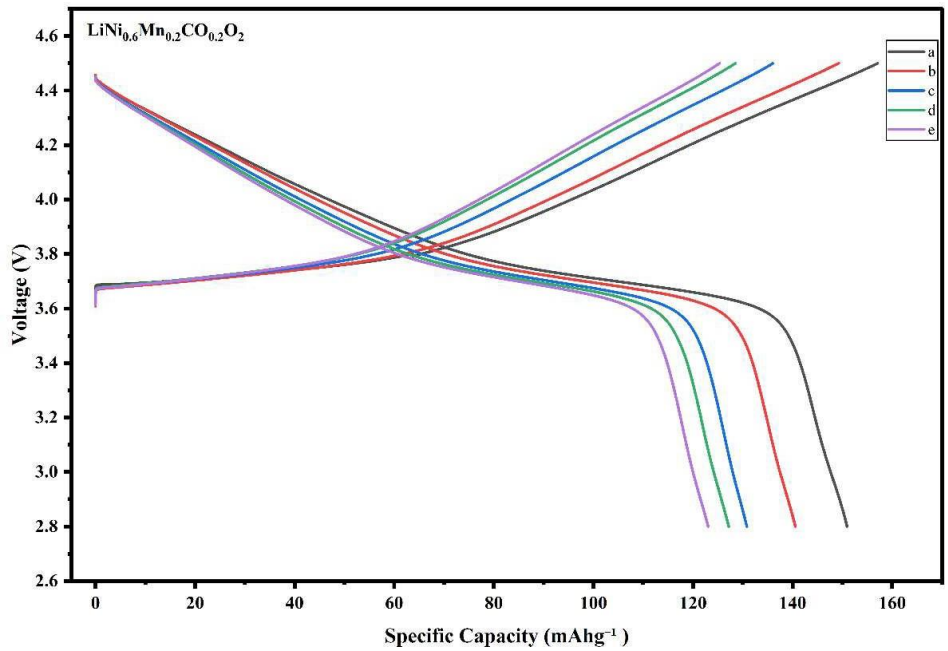

Figure 9: GCD graph of Pristine NMC622

The pristine $LiNi_{0.6}Mn_{0.2}Co_{0.2}O_2$ cathode show an initial charge capacity of 157.10 mAh g^{-1} and a corresponding discharge capacity of 150.95 mAh g^{-1} during the first cycle and this relative high initial discharge capacity of the pristine sample can be attributed mainly to the larger nickel concentration within the layered structure. As we know that in Ni-rich layered oxide cathodes nickel contributes significantly toward electrochemical capacity through the reversible oxidation and reduction of Ni^{2+}/Ni^{4+} during lithium extraction and insertion [39]. So higher the nickel concentration in the sample generally gives enhanced initial discharge capacity.

Still it was noticed that despite having comparatively higher initial capacity, the pristine NMC622 sample showed rapid capacity fading during subsequent cycling. For example the discharge capacity decreased continuously from 150.95 mAh g^{-1} in the first cycle to 140.47 mAh g^{-1} in the second cycle and then followed by further reduction to 130.82, 127.19, and finally 123.05 mAh g^{-1} by the fifth cycle and such type of electrochemical degradation is commonly observed in Ni-rich layered oxide

cathodes and it is mainly associated with structural instability arising during repeated lithium extraction and insertion processes while charging and discharging[40].

Several degradation mechanisms have been proposed in the literature for explaining the rapid capacity decay of Ni-rich layered cathodes. For example when charging the cathode material to high voltages, especially above 4.3 V some partial destabilization of the layered lattice takes place because of the excessive lithium extraction from the crystal framework [38] and due to this destabilization the movement of transition metal ions, particularly Ni^{2+}, TM layers into lithium layers. Also the resulting Li^{+}/Ni^{2+} cation mixing in the Pristine NMC622 cathode blocks the lithium diffusion pathways and hence increases electrochemical polarization during cycling [21], Also at the same time, repeated lithium extraction also generates lattice strain because of anisotropic contraction and expansion of the crystal structure and such structural stress eventually accelerates particle cracking and degradation of the cathode material [41]. Another one of the important degradation mechanism in Ni-rich cathodes is surface reconstruction. As seen in the previous studies the outer surface of layered oxide cathodes gradually transforms into spinel-like or rock-salt phases during repeated cycling [40]. These reconstructed surface layers possess comparatively poor lithium-ion conductivity and therefore increase charge transfer resistance and hence reduced capacity in the further consecutive cycles. Surface degradation also enhances extra reactions between the cathode and electrolyte, resulting in electrolyte decomposition and irreversible lithium consumption and along with that, although pristine NMC622 exhibits relatively high initial capacity, its electrochemical stability decreases rapidly during repeated cycling because of structural and interfacial degradation[41].

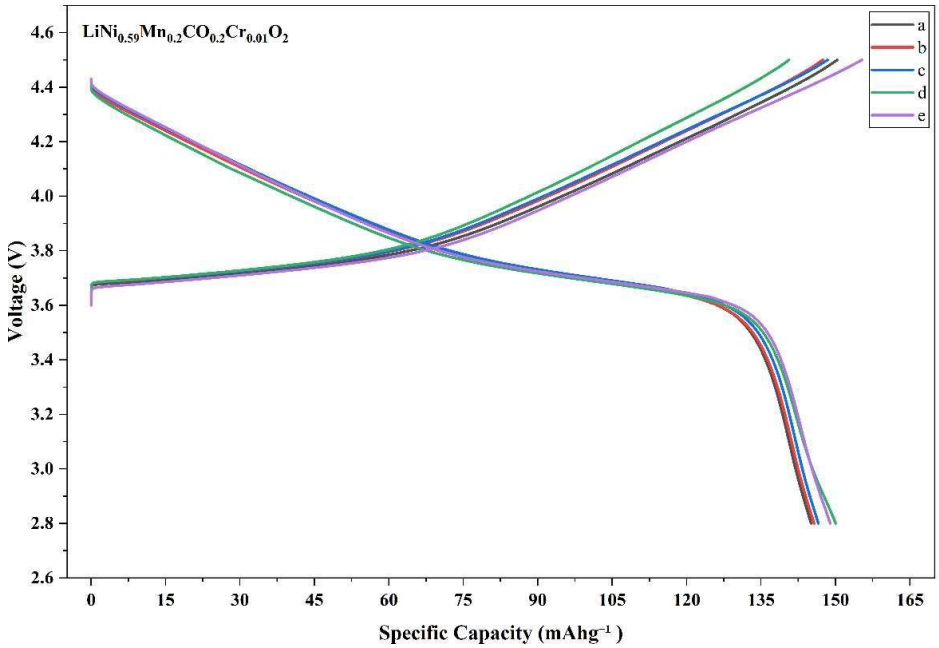

Figure 10: GCD graph of $LiNi_{0.59}Mn_{0.2}CO_{0.2}Cr_{0.01}O_2$

After chromium substitution, noticeable changes in electrochemical behaviour were observed. The 1% Cr-doped sample, $LiNi_{0.59}Mn_{0.2}Co_{0.2}Cr_{0.1}O_2$, exhibited an initial charge capacity of 150.36 mAh g^{-1} and an initial discharge capacity of 145.08 mAh g^{-1} and although the initial discharge capacity was slightly lower compared to pristine NMC622, the cycling behaviour appeared considerably more stable, also interestingly, instead of continuous capacity fading, the discharge capacity showed a gradual increase during the initial cycles. The discharge capacity increased from 145.08 mAh g^{-1} during the first cycle to 145.68 mAh g^{-1} in the second cycle, followed by 146.54 mAh g^{-1} in the third cycle and approximately 150.04 mAh g^{-1} during the fourth cycle before slightly decreasing to 148.94 mAh g^{-1} in the fifth cycle.

Looking at it first, such an increase in discharge capacity during cycling may appear unusual, however, similar electrochemical activation behaviour has been widely reported in layered oxide cathodes during the initial cycles [42] . It is studied that during early cycling, gradual electrolyte penetration into the porous electrode structure improves the accessibility of electrochemically active sites and simultaneously, stabilization of the electrode/electrolyte interface and redistribution of lithium ions within the layered framework can enhance lithium diffusion kinetics [21]. As a result,

the discharge capacity may increase slightly during the first few cycles before eventually stabilizing. Another possible reason behind this activation behaviour is the stabilization effect induced by chromium substitution as chromium ions possess stronger Cr-O bonding interactions compared to Ni-O bonds [23] which help stabilize the ransitionn metal layers and suppress migration of transition metal ions during repeated cycling. Consequently, moderate chromium substitution reduces structural degradation and improves cycling retention. Similar improvements in cycling stability after chromium doping have been reported previously in several Cr-doped layered oxide systems [21], [22].

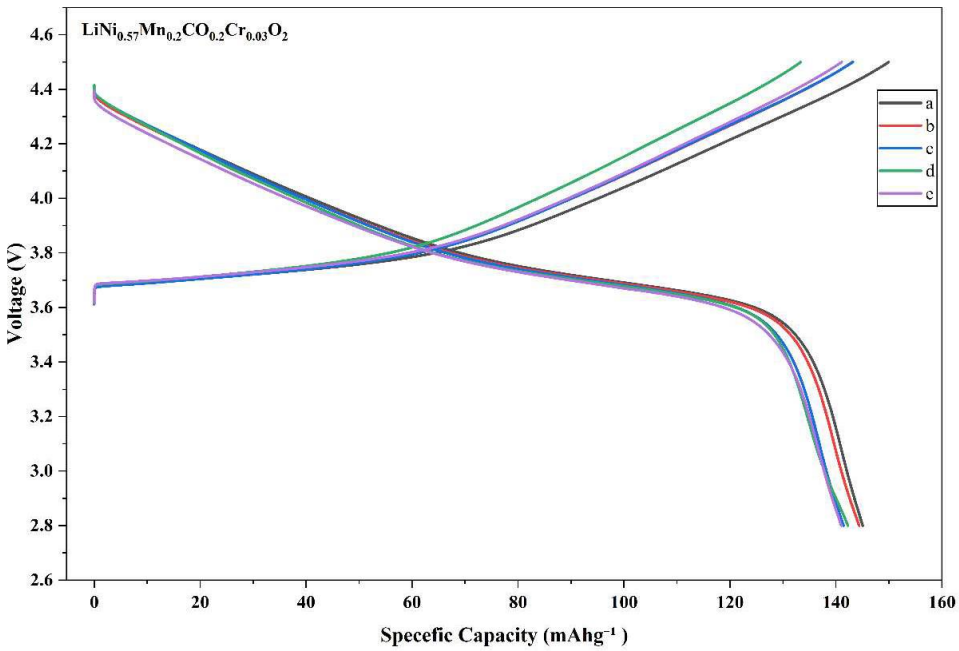

Figure 11: GCD graph of $LiNi_{0.57}Mn_{0.2}CO_{0.2}Cr_{0.03}O_2$

The electrochemical behaviour of the 3% Cr-doped sample, $LiNi_{0.57}Mn_{0.2}Co_{0.2}Cr_{0.3}O_2$, was slightly different as compared to 1% Cr-doped sample. The sample shows an initial discharge capacity of 145.04 mAh g^{-1} and kept comparatively stable capacities around 141-144 mAh g^{-1} throughout the first five cycles. Als compared to the pristine sample, the 3% Cr-doped composition showed significantly improved capacity

retention. However, unlike the 1% Cr-doped sample, no major activation-related increase in capacity was observed during cycling. This behaviour indicates that higher chromium concentration further stabilizes the layered framework but simultaneously reduces the amount of electrochemically active nickel ions participating in the redox process [21]. Also since chromium itself contributes very little toward reversible lithium storage so replacing excessive nickel with chromium decreases the total discharge capacity of the material and therefore, the electrochemical performance of Cr-doped NMC622 cathodes depends strongly on achieving an optimum balance between structural stabilization and electrochemical activity.

Also the coulombic efficiency of the synthesized cathodes was also calculated during each cycle and the pristine sample exhibited an initial coulombic efficiency of approximately 96.08%, whereas the 1% and 3% Cr-doped samples showed initial efficiencies of approximately 96.48% and 96.74%, respectively. The relatively high coulombic efficiency values indicate good reversibility of lithium insertion and extraction reactions in all synthesized cathodes but slight improvement in coulombic efficiency after chromium substitution may indicate suppression of irreversible side reactions occurring at the cathode/electrolyte interface [43]. Another noticeable feature is seen in Cr-doped samples in the charge-discharge curves, as the slight overlap and intersection between certain discharge profiles. Also in practical electrochemical systems, especially during low-cycle measurements, such intersections are not uncommon [41]. Certain parameters can show variations in polarization, redistribution of lithium ions, electrode wetting behaviour, and stabilization of the solid electrolyte interphase, which can slightly alter the relative positions of consecutive charge-discharge curves. Therefore, minor curve intersections should not be considered abnormal electrochemical behaviour.

The electrochemical observations obtained from GCD measurements are also supported by the structural analysis performed using X-ray diffraction as all the synthesized samples are crystallized in the layered hexagonal α-$NaFeO_2$ structure without any detectable impurity peaks which confirms the successful synthesis of phase-pure layered cathodes[42].

Interestingly, despite exhibiting lower cation mixing, the pristine sample did not show the best cycling stability so this shows we cannot explain the electrochemical performance only on the basis of cation mixing because it does also depends on other parameters as well and also the lower cation mixing generally improves lithium diffusion kinetics but with it chromium doping simultaneously enhances structural stability of the material and also reduce the degradation mechanisms that is associated with high-voltage cycling in the pristine sample[21] and therefore the final electrochemical behaviour of our material is due to structural stability, transition metal redox activity, lithium diffusion kinetics along with the interfacial stability. So we can say that the overall our electrochemical results shows that the chromium doping significantly improve the cycling behaviour of pristine NMC622 cathodes, also the moderate chromium doping improves structural stability and reduce rapid capacity fading during repeated cycling and excessive chromium doping reduces the reversible discharge capacity because of the reduced nickel present in the material and hence gives better electrochemical redox process. Also among all synthesized compositions, the 1% Cr-doped sample shows comparatively balanced electrochemical performance with improved cycling stability and reasonable discharge capacity retention and the obtained results therefore suggest that optimized chromium substitution can effectively enhance the electrochemical stability of layered NMC622 cathode materials for lithium-ion battery applications.

CHAPTER 5

CONCLUSIONS AND FUTURE SCOPE

5.1 Conclusion

Our work focused on the synthesis and electrochemical investigation of Cr-doped NMC622 cathode materials for LIBs applications and the materials were synthesized using the sol-gel method and calcinated at 900 °C where different chromium concentrations were introduced into the NMC622 structure in order to find the influence of Cr substitution on structural stability and electrochemical behaviour. XRD analysis shows that a layered hexagonal α-$NaFeO_2$ structure is with rhombohedral symmetry for all synthesized samples is formed and also there were no extra impurity peaks is observed in the diffraction patterns, so it indicates that the incorporation of chromium within the layered lattice is successful without disturbing the overall crystal structure of the material. Along with that the clear splitting of the doublets peaks also suggested the good layered ordering in the synthesized cathode materials and apart from that the cation mixing, that was calculated using the I(003)/I(104) intensity ratio showed the noticeable variation in capacity and structural stability with chromium concentration. Also a decrease in this ratio was observed with chromium substitution, that suggests the partial modification in cation distribution within the layered framework. Also, the electrochemical behaviour of the doped sample shows that cation mixing is not the only parameter that govern the discharge capacity of the material because other factors also play the important rols in determining the overall battery performance such as lattice stabilization, transition metal interactions, lithium diffusion kinetics, and structural retention during cycling.

GCD studies that was performed in the voltage window of 2.5-4.5 V at 0. 1 C the distinct electrochemical behaviour for the pristine and chromium-doped samples as the pristine material showed a relatively higher initial discharge capacity, but also faster capacity fading during subsequent cycles also the 1% Cr-doped sample shows comparatively better cycling stability with more stable discharge capacities over the repeated cycles and this behaviour suggests that controlled chromium substitution may

help in stabilizing the layered structure during lithium extraction and insertion processes. Also the 3% chromium-doped sample however having comparatively lower discharge capacity that indicate that excessive chromium substitution may reduce electrochemically active nickel content and increase structural polarization. This observation highlights the importance of optimizing dopant concentration rather than simply increasing dopant amount. The obtained results therefore suggest that moderate chromium incorporation can improve structural stability, whereas excessive substitution may adversely influence lithium-ion diffusion and charge transfer processes.

SEM analysis of the pristine sample revealed strongly agglomerated primary particles forming dense secondary structures, which is a characteristic morphology commonly observed in layered oxide cathode materials synthesized by the sol-gel route and such morphology may contribute toward better particle connectivity, although excessive agglomeration can also influence electrolyte penetration and diffusion behaviour during electrochemical cycling. Overall, the present study indicates that chromium doping can influence both structural and electrochemical properties of NMC622 cathode materials. While the pristine sample delivered relatively high initial discharge capacity, the chromium-doped compositions exhibited improved capacity retention behaviour during cycling. Among the investigated compositions, the 1% chromium-doped sample demonstrated the most balanced electrochemical performance, suggesting that controlled Cr substitution may be an effective strategy for improving the cycling stability of layered NMC cathodes for lithium-ion battery applications.

5.2 Future Scope

Although the present work demonstrates the effect of chromium doping on NMC622 cathode materials, several aspects still remain open for further investigation. The electrochemical behaviour of layered oxide cathodes is highly complex and depends simultaneously on crystal structure, particle morphology, dopant distribution, surface chemistry, and electrode-electrolyte interactions, therefore, a more detailed understanding of these factors would be useful for improving the long-term performance of chromium-doped cathode materials.

In the present work, electrochemical characterization was primarily limited to galvanostatic charge-discharge analysis. Further studies involving cyclic voltammetry and EIS may provide deeper insight into charge transfer resistance, lithium-ion diffusion kinetics, polarization behaviour, and electrode stability during prolonged cycling of the cathode material that would help in understanding how chromium substitution influences electrochemical reaction mechanisms at different states of charge. Also some other advanced structural characterization techniques such as XPS, TEM, Raman spectroscopy, and in situ XRD may be used in future work to investigate surface reconstruction, oxidation state variation, transition metal migration, and structural evolution during repeated charge-discharge cycles along with the SEM of the doped sample to study morphology as these analyses can provide more direct evidence regarding the stabilization effect of chromium within the layered oxide framework and with that another important direction for future research involves the optimization of chromium doping because the present results suggest that the moderate chromium doping improves cycling stability but excessive doping may reduce electrochemical activity because of decreased nickel participation and therefore investigating the intermediate chromium doping may help to identify a good balance between structural stability and discharge capacity. Also coating materials such as Li_3PO_4, AlO_3, Zr_2O_2, or conductive carbon layers can be used as surface modification along with chromium doping in future studies which could potentially reduce electrolyte decomposition and surface degradation at high voltages so combining surface coating with elemental doping may further improve thermal stability and long-term cycling performance of NMC622 cathodes.

Also in the future work some additional synthesis parameters and their influence can be explored such as calcination temperature, heating rate, precursor chemistry and atmosphere control on particle morphology and electrochemical performance as layered oxide cathodes are highly sensitive to synthesis conditions so even a small variations during the preparation of the cathode material can significantly alter cation ordering and structural stability. Also based on our work it can be said that chromium-doped NMC622 materials remain a very promising candidates because of their ability to combine relatively high discharge capacity with improved structural stability in the cathode material.

REFRENCES

[1] M. A. Wicaksono et al., "Advanced engineering of Nd-doped LiNMC hybrid supercapacitor materials with planetary ballmill method and DEM-based microstructural simulation," Next Materials, vol. 9, p. 100987, Oct. 2025, doi: https://doi.org/10.1016/j.nxmate.2025.100987.

[2] "Overview of Lithium-ion Battery Components: Anode & Cathode," Redwoodmaterials.com, Jul. 02, 2024. https://www.redwoodmaterials.com/resources/cathode-and-anode/ (accessed Dec. 08, 2024).

[3] K. R. Ngoy et al., "Lithium-ion batteries and the future of sustainable energy: A comprehensive review," Renewable and Sustainable Energy Reviews, vol. 223, p. 115971, Jul. 2025, doi: https://doi.org/10.1016/j.rser.2025.115971.

[4] B. E. Murdock, K. E. Toghill, and N. Tapia-Ruiz, "A Perspective on the Sustainability of Cathode Materials used in Lithium-Ion Batteries," Advanced Energy Materials, vol. 11, no. 39, p. 2102028, Sep. 2021, doi: https://doi.org/10.1002/aenm.202102028.

[5] B. Rani, J. K. Yadav, P. Saini, and A. Dixit, "LiMn2O4 as a cathode material: challenges and opportunities for lithium-ion batteries," Sustainable Energy & Fuels, vol. 9, no. 16, pp. 4262–4285, 2025, doi: https://doi.org/10.1039/d5se00565e.

[6] Z. Bao et al., "Effects of transition metal doping on electrochemical properties of single-crystalline LiNi0.7Co0.1Mn0.2O2 cathode materials for lithium-ion batteries," Journal of Alloys and Compounds, vol. 872, pp. 159619–159619, Aug. 2021, doi: https://doi.org/10.1016/j.jallcom.2021.159619.

[7] C. Xu, P. J. Reeves, Q. Jacquet, and C. P. Grey, "Phase Behavior during Electrochemical Cycling of Ni-Rich Cathode Materials for Li-Ion Batteries,"

Advanced Energy Materials, vol. 11, no. 7, Dec. 2020, doi: https://doi.org/10.1002/aenm.202003404.

[8] Z. Pei et al., "Effects of Cr3+ Doping on Spinel LiMn2O4 Morphology and Electrochemical Performance," International Journal of Molecular Sciences, vol. 25, no. 24, p. 13270, Dec. 2024, doi: https://doi.org/10.3390/ijms252413270.

[9] C. P. Woodley, P. Mondol, R. A. Cooper, and B. M. Bartlett, "Tetrahedral Zn2+ doping LiNi0.6Mn0.2Co0.2O2 improves discharge capacity retention by altering surface Ni valence during cycling and preventing oxygen evolution," Journal of Power Sources, vol. 676, p. 239779, Jun. 2026, doi: https://doi.org/10.1016/j.jpowsour.2026.239779.

[10] J. Zhu, G. Xiao, and X. Li, "Synthesis of Li(Ni0.6Co0.2Mn0.2)O2 by a modified sol-gel method for lithium-ion batteries," Synthetic Metals, vol. 281, p. 116905, Nov. 2021, doi: https://doi.org/10.1016/j.synthmet.2021.116905.

[11] Oyunbayar Nyamaa, G.-H. Kang, S.-C. Huh, J.-H. Yang, T.-H. Nam, and J.-P. Noh, "Unraveling the Mechanism and Practical Implications of the Sol-Gel Synthesis of Spinel LiMn2O4 as a Cathode Material for Li-Ion Batteries: Critical Effects of Cation Distribution at the Matrix Level," Molecules, vol. 28, no. 8, pp. 3489–3489, Apr. 2023, doi: https://doi.org/10.3390/molecules28083489.

[12] J. B. Goodenough and K.-S. Park, "ChemInform Abstract: The Li-Ion Rechargeable Battery: A Perspective," ChemInform, vol. 44, no. 20, p. no-no, Apr. 2013, doi: https://doi.org/10.1002/chin.201320273.

[13] K. Akhmetova, F. Sultanov, A. Mentbayeva, Z. Bakenov, and B. Tatykayev, "Review on the dimensionality (0D 3D) of NCM cathode morphologies: Impact on electrochemical performance in lithium-ion batteries," Journal of Energy Storage, vol. 154, p. 121289, Apr. 2026, doi: https://doi.org/10.1016/j.est.2026.121289.

[14]A. Rougier, C. Delmas, and A. V. Chadwick, "Non-cooperative Jahn-Teller effect in LiNiO2: An EXAFS study," Solid State Communications, vol. 94, no. 2, pp. 123–127, Apr. 1995, doi: https://doi.org/10.1016/0038-1098(95)00020-8.

[15] Z. Xu et al., “Layered oxide cathodes: A comprehensive review of characteristics, research, and development in lithium and sodium ion batteries,” Carbon Neutralization, Aug. 2024, doi: https://doi.org/10.1002/cnl2.162.

[16] J. Wang et al., “Doping Strategy in Nickel-Rich Layered Oxide Cathode for Lithium-Ion Battery,” Renewables, pp. 1–25, May 2023, doi: https://doi.org/10.31635/renewables.023.202200022.

[17] W.-T. Lo, C. Yu, E. G. Leggesse, S. Nachimuthu, and J.-C. Jiang, “Understanding the Role of Dopant Metal Atoms on the Structural and Electronic Properties of Lithium-Rich Li1.2Ni0.2Mn0.6O2 Cathode Material for Lithium-Ion Batteries,” The Journal of Physical Chemistry Letters, vol. 10, no. 17, pp. 4842–4850, Aug. 2019, doi: https://doi.org/10.1021/acs.jpclett.9b01516.

[18] Songyoot Kaewmala et al., “Impacts of Mg doping on the structural properties and degradation mechanisms of a Li and Mn rich layered oxide cathode for lithium-ion batteries,” Scientific reports, vol. 13, no. 1, Mar. 2023, doi: https://doi.org/10.1038/s41598-023-31492-0.

[19] J. Fan, C. Cao, L. Shang, and L. Yuan, “Structural stabilization effect of Mg-Al co-doping on high-nickel layered cathode material LiNi0.9Co0.1O2,” Journal of Power Sources, vol. 658, p. 238336, Dec. 2025, doi: https://doi.org/10.1016/j.jpowsour.2025.238336.

[20] M. Zybert et al., “Structural analysis and electrochemical investigation of dual-doped NMC622 cathode material: Effect of sodium and neodymium on the performance in Li-ion batteries,” Energy Reports, vol. 10, pp. 1238–1248, Nov. 2023, doi: https://doi.org/10.1016/j.egyr.2023.07.061.

[21] L. Sun, L. Zhu, C. Mi, E. Han, M. Shang, and Z. Zeng, “The effects of Cr substitution on LiNi0.65Co0.1Mn0.25O2 for lithium-ion batteries,” Ionics, vol. 25, no. 7, pp. 3021–3030, Feb. 2019, doi: https://doi.org/10.1007/s11581-019-02900-1.

[22] U. Nisar et al., “Synthesis and electrochemical characterization of Cr-doped lithium-rich Li1.2Ni0.16Mn0.56Co0.08-xCrxO2 cathodes,” Emergent Materials, vol. 1, no. 3–4, pp. 155–164, Oct. 2018, doi: https://doi.org/10.1007/s42247-018-0014-0.

[23] M. Wang, Y. Chen, F. Wu, Y. Su, and L. Chen, "Improvement of the electrochemical performance of LiNi0.33Mn0.33Co0.33O2 cathode material by chromium doping," Science China Technological Sciences, vol. 53, no. 12, pp. 3214–3220, Nov. 2010, doi: https://doi.org/10.1007/s11431-010-4155-5.

[24] F. I. Saaid et al., "Ni-rich lithium nickel manganese cobalt oxide cathode materials: A review on the synthesis methods and their electrochemical performances," Heliyon, vol. 10, no. 1, p. e23968, Jan. 2024, doi: https://doi.org/10.1016/j.heliyon.2023.e23968.

[25] F. Li et al., "Ni-Rich Layered Oxide with Preferred Orientation (110) Plane as a Stable Cathode Material for High-Energy Lithium-Ion Batteries," Nanomaterials, vol. 10, no. 12, p. 2495, Dec. 2020, doi: https://doi.org/10.3390/nano10122495.

[26] Z. Chen et al., "Hierarchical Porous LiNi1/3Co1/3Mn1/3O2 Nano-/Micro Spherical Cathode Material: Minimized Cation Mixing and Improved Li+ Mobility for Enhanced Electrochemical Performance," Scientific Reports, vol. 6, no. 1, May 2016, doi: https://doi.org/10.1038/srep25771.

[27] A. L. Lipson et al., "Improving the Thermal Stability of NMC 622 Li-Ion Battery Cathodes through Doping During Coprecipitation," ACS Applied Materials & Interfaces, vol. 12, no. 16, pp. 18512–18518, Apr. 2020, doi: https://doi.org/10.1021/acsami.0c01448.

[28] B. Zhang, L. Wang, H. Zhang, H. Xu, and X. He, "Revelation of the transition-metal doping mechanism in lithium manganese phosphate for high performance of lithium-ion batteries," Battery Energy, vol. 1, no. 4, p. 20220020, Sep. 2022, doi: https://doi.org/10.1002/bte2.20220020.

[29] Hashem et al., "Doped Nanoscale NMC333 as Cathode Materials for Li-Ion Batteries," Materials, vol. 12, no. 18, p. 2899, Sep. 2019, doi: https://doi.org/10.3390/ma12182899.

[30] M. Colalongo et al., "Comprehensive Study of Zr-Doped Ni-Rich Cathode Materials Upon Lithiation and Co-Precipitation Synthesis Steps," ACS Applied

Materials & Interfaces, vol. 16, no. 22, pp. 28683–28693, May 2024, doi: https://doi.org/10.1021/acsami.4c05058.

[31] M. M. Thackeray and K. Amine, "Layered Li–Ni–Mn–Co oxide cathodes," Nature Energy, vol. 6, no. 9, pp. 933–933, Sep. 2021, doi: https://doi.org/10.1038/s41560-021-00860-3.

[32] Z. Meng, X. Ma, L. Azhari, J. Hou, and Y. Wang, "Morphology controlled performance of ternary layered oxide cathodes," Communications Materials, vol. 4, no. 1, pp. 1–15, Nov. 2023, doi: https://doi.org/10.1038/s43246-023-00418-8.

[33] X. Jiang, L. Qin, H. Yu, L. Chen, H. Jiang, and C. Li, "All-Dry Synthesis of Single-Crystalline LiNi0.6Mn0.2Co0.2O2 Cathodes for High-Energy and Long-Life Li-Ion Batteries," Industrial & Engineering Chemistry Research, vol. 63, no. 23, pp. 10291–10298, May 2024, doi: https://doi.org/10.1021/acs.iecr.4c01424.

[34] M. H. Tahmasebi and M. N. Obrovac, "New Insights into the All-Dry Synthesis of NMC622 Cathodes Using a Single-Phase Rock Salt Oxide Precursor," ACS Omega, vol. 9, no. 1, pp. 1916–1924, Dec. 2023, doi: https://doi.org/10.1021/acsomega.3c08702.

[35] L. Zou et al., "The Role of Secondary Particle Structures in Surface Phase Transitions of Ni-Rich Cathodes," Chemistry of materials, vol. 32, no. 7, pp. 2884–2892, Mar. 2020, doi: https://doi.org/10.1021/acs.chemmater.9b04938.

[36] J. Z. Olson, C. M. López, and Edmund, "Differential Analysis of Galvanostatic Cycle Data from Li-Ion Batteries: Interpretative Insights and Graphical Heuristics," *Chemistry of materials*, vol. 35, no. 4, pp. 1487–1513, Feb. 2023, doi: https://doi.org/10.1021/acs.chemmater.2c01976.

[37] J. Li, E. Murphy, J. Winnick, and P. A. Kohl, "The effects of pulse charging on cycling characteristics of commercial lithium-ion batteries," *Journal of Power Sources*, vol. 102, no. 1, pp. 302–309, Dec. 2001, doi: https://doi.org/10.1016/S0378-7753(01)00820-5.

[38] F. Lin et al., “Surface reconstruction and chemical evolution of stoichiometric layered cathode materials for lithium-ion batteries,” Nature Communications, vol. 5, no. 1, p. 3529, Mar. 2014, doi: https://doi.org/10.1038/ncomms4529.

[39] A. L. Lipson *et al.*, “Improving the Thermal Stability of NMC 622 Li-Ion Battery Cathodes through Doping During Coprecipitation,” *ACS Applied Materials & Interfaces*, vol. 12, no. 16, pp. 18512–18518, Apr. 2020, doi: https://doi.org/10.1021/acsami.0c01448.

[40] H. Zheng, Q. Sun, G. Liu, X. Song, and V. Battaglia, “Correlation between dissolution behavior and electrochemical cycling performance for LiNi1/3Co1/3Mn1/3O2-based cells,” *Journal of Power Sources*, vol. 207, pp. 134–140, Jun. 2012, doi: https://doi.org/10.1016/j.jpowsour.2012.01.122.

[41] F. Licht, M. M. Davis, and H. A. Andreas, “Charge redistribution and electrode history impact galvanostatic charging/discharging and associated figures of merit,” *Journal of Power Sources*, vol. 446, pp. 227354–227354, Jan. 2020, doi: https://doi.org/10.1016/j.jpowsour.2019.227354.

[42]T. Zhao *et al.*, “The effect of chromium substitution on improving electrochemical performance of low-cost Fe–Mn based Li-rich layered oxide as cathode material for lithium-ion batteries,” *Journal of Power Sources*, vol. 245, pp. 898–907, Jan. 2014, doi: https://doi.org/10.1016/j.jpowsour.2013.07.026.

[43]L. Liu, K. Sun, N. Zhang, and T. Yang, “Improvement of high-voltage cycling behavior of Li(Ni1/3Co1/3Mn1/3)O2 cathodes by Mg, Cr, and Al substitution,” Journal of Solid State Electrochemistry, vol. 13, no. 9, pp. 1381–1386, Oct. 2008, doi: https://doi.org/10.1007/s10008-008-0695-z.